

# Measurement of corrosion behaviour of magnesium alloys developed for application in biomaterials area

L. Joska<sup>1\*</sup>, B. Smola<sup>2</sup>, I. Stulíková<sup>2</sup>, F. Hnilica<sup>3</sup>

<sup>1</sup>*Institute of Chemical Technology in Prague, Faculty of Chemical Technology,  
Technická 5, 166 28 Prague 6, Czech Republic*

<sup>2</sup>*Charles University in Prague, Faculty of Mathematics and Physics, Ke Karlovu 3, 121 16 Prague 2, Czech Republic*

<sup>3</sup>*Czech Technical University in Prague, Faculty of Mechanical Engineering,  
Karlovo náměstí 13, 121 35 Prague 2, Czech Republic*

Received 9 April 2013, received in revised form 6 November 2013, accepted 11 March 2014

## Abstract

The use of magnesium alloys is very interesting for orthopaedic applications. Corrosion rate of these materials can be determined by a range of techniques. The study was aimed at the assessment the ability of electrochemical methods to provide comparable results. Corrosion behaviour study was composed of polarisation resistance and electrochemical impedance spectra measurements as well as release of hydrogen detection. An apparatus for measurement of the volume of released hydrogen under clearly defined conditions was designed. Based on results it is possible to conclude: measurement of electrochemical impedance spectra provides information on the system behaviour in each phase of exposure. The data can be used to determine both the development of all resistances and the layer resistance. This represents an important advantage compared to the polarisation resistance determined by DC technique. The quality of corrosion behaviour assessment would substantially be increased by comparing results of several methods.

**Key words:** magnesium alloy, corrosion, electrochemistry, hydrogen

## 1. Introduction

The use of magnesium alloys is a widely discussed topic. This group of materials seems to be very interesting for orthopaedic applications [1], even though they have been applied only as stents so far [2]. The main goal of the research is to achieve a corrosion rate that would enable a “programmable” service-life of implants and would not cause potential issues with released hydrogen and/or corrosion products [3–5].

Magnesium and its alloys represent a group of materials the corrosion of which can be determined by a wide range of techniques; however, the results of *in vitro* tests often markedly differ from the values measured during *in vivo* exposures [6]. The usually applied laboratory procedure is the corrosion rate determination based on weight changes. The method specific for this system is measurement of the corrosion rate based on detection of the volume of released hydrogen – that

means on the rate of cathodic reaction. In addition to these techniques a set of electrochemical procedures is available – the same as for other corroding metallic materials. It is a method for corrosion rate determination based on extrapolation of linear parts of potentiodynamic curves (so called Tafel test), polarisation resistance determination and the electrochemical impedance spectra measurement. Kirkland et al. [7] have recently published a review article on measurement techniques based on a large number of references. The analysis of literature data implies that results interpretation may be ambiguous, considering special features of the studied system’s behaviour. The corrosion rate values determined electrochemically, on the base of weight changes and volume of released hydrogen may differ significantly [7–11]. The differences are explained by the surface being shielded by hydrogen, dissolution of hydrogen in the specimen, non-uniformity of the attack and electrochemical oxidation of mag-

\*Corresponding author: tel.: +420220444204; fax: +420220444400; e-mail address: [Ludek.Joska@vscht.cz](mailto:Ludek.Joska@vscht.cz)

Table 1. Composition of studied alloys, production technology and heat treatment (C – cast, PM – powder metallurgy)

Element (wt.%)	Mg	Y	Gd	Ce	Nd	Sc	Mn	Zr	Zn	Tb	Production technology	Cast – heat treatment T5
A; A1	95.11			2.84		0.92	1.16				A = cast	A1=275/42
B	94.20			3.72			1.16		0.92		cast	
C; C1	88.16		9.63			0.91	1.3				C = cast	C1=200/72
D; D1	93.57		4.64			0.26	1.53				D = cast	D1=200/96
E1	90.45	5.2	1.61		2.42			0.32			PM	extrusion 250 °C
E2	90.45	5.2	1.61		2.42			0.32			PM	extrusion 400 °C
F; F1	97.71	3.71			2.12	1.28	4.18				F = cast	F1 = 200/45
F2	92.21	3.31			2.90	0.62	0.96				PM	extrusion 280 °C
G	91.99	3.22			2.12		1.45				cast	
H	92	2			1				1.22		PM	extrusion 280 °C
I	94				2					4	cast	
I1	93.7				2.5					3.8	PM	extrusion 250 °C
J; J1	94.18	3.88				0.83	1.11		1		J = cast	J1 = 275/48
K	93.8	3.88					1.13		1.19		cast	
Mg	99.95											

nesium to both  $Mg^{2+}$  and  $Mg^+$  ions. The existence of  $Mg^+$  ion as a semi-product of the corrosion reaction is already referred to in works [12, 13].

This study, which is a part of a larger study dealing with corrosion behaviour of magnesium and its alloys alloyed with rare earth elements, manganese and zinc, is aimed at the assessment the ability of electrochemical experimental approaches to provide comparable results.

## 2. Experimental

The tests were conducted using a set of specimens prepared by pressure casting or powder metallurgy technology (Table 1). Behaviour of cast alloys was studied in the state after casting or after heat treatment T5 (Table 1, the specimens were quenched in water after annealing), after which the maximum strength was achieved. The alloys prepared by powder metallurgy (PM) were studied after extrusion with no further heat treatment. Corrosion behaviour of magnesium was measured on specimens with a declared purity of 99.93 wt.%. Cylindrical specimens 8 mm in diameter and 20 mm in length were made out of the semi-products. Before testing, the surface was ground (P1200), washed with distilled water and ethyl alcohol.

The exposures proceeded in physiological solution ( $9\text{ g l}^{-1}$  sodium chloride) at  $37^\circ\text{C}$ . This model of a body environment contains only the aggressive (chloride) components; hence the measurement could not have been influenced by an interaction of corrosion products with the model environment (e.g., phosphates in buffered saline solution) or precipitation of insoluble salts from the model environment (e.g., hydroxyapatite in simulated body fluid). Corrosion be-

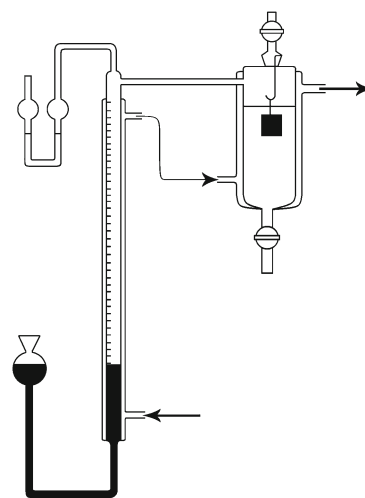


Fig. 1. Experimental setup used for the release of hydrogen measurement.

haviour was assessed on the base of 3 types of experimental approaches.

### 2.1. Hydrogen release rate measurement

The principle of the device used for the purpose of corrosion rate measurement based on the volume of gas released by a cathodic reaction is presented in Fig. 1. Considering the necessity to eliminate potential hydrogen leaks, all components of the glass apparatus were connected with ball joints. Decane and mercury were used as a closing liquid in a manometric tube and burette, respectively. The temperature in the whole system was sustained at  $37^\circ\text{C}$  by a water bath. The connection between the exposure cell and the gasometric burette was covered by thermal

insulation. The burette had a volume of 10 ml divided in steps of 0.05 ml. After filling the tempered cell with physiological solution (37°C) saturated with hydrogen, the system was thermally equilibrated for 30 min before the specimen was inserted. The specimen hanging on a Teflon fibre was placed in the upper third of the exposure cell. The 24-hour exposures were done. The volume of released hydrogen was recorded in two phases – for 4 to 5 h in the beginning of the exposure (1<sup>st</sup> phase), and for 4 to 5 h at the end (2<sup>nd</sup> phase). In the meantime, the system was open and hydrogen was freely evolved to the atmosphere.

## 2.2. Polarisation resistance measurement

Open circuit potential ( $E_{\text{ocp}}$ ) and polarisation resistance ( $R_{\text{pDC}}$ ) measured at  $\pm 20 \text{ mV}/E_{\text{ocp}}$  with the potential change rate of  $0.1 \text{ mV s}^{-1}$  were recorded for 24 h with a 1-hour periodicity. In order to determine  $R_{\text{pDC}}$ , the range of  $\pm 10 \text{ mV}$  from the open circuit potential was chosen. Polarisation resistance was calculated as  $\Delta E/\Delta j$ , unit of this quantity is  $\Omega \text{ m}^2$ . Reference 600 potentiostat (Gamry) was used for measurements.

## 2.3. Electrochemical impedance spectra measurement

Electrochemical impedance spectra (EIS) were

measured at the open circuit potential in frequency range from 50 kHz to 25 mHz, for 24 h with a 1-hour periodicity. One measurement took approximately 14 min. Reference 600 potentiostat (Gamry) was used for measurements.

The originally planned determination of weight changes of specimens proved to be unfeasible. Considering their size and time of exposure, weight changes were very small to be precisely detected by analytical balances and removal of corrosion products (specimens frequently showed a deep corrosion attack) could influence subsequent measurements.

The state of surface was photographed after exposures; a few specimens were subjected to the photoelectron spectroscopy analysis (XPS) (EscaProbe P spectrometer, Omicron). Both the survey spectra within the binding energy range 0–580 eV (step 0.2 eV, pass energy 50 eV) and detailed spectra corresponding to binding energies of particular alloying elements (step 0.05 eV, pass energy 25 eV) were scanned in this case. Concentration profiles were obtained by surface sputtering with argon ions beam. The sputtering rate was calibrated using a magnesium specimen. The depths of etch pits were determined by the AFM microscope (CP-II, Veeco) and profilometer (SurfTest SJ-301, Mitutoyo).

The electrochemical data were processed by Echem Analyst programme (Gamry), XPS spectra were analysed by CasaXPS software (Casa Software).

Table 2. Polarisation resistance calculated from release of hydrogen rate ( $R_{\text{pVOL}}$ ), based on DC measurement ( $R_{\text{pDC}}$ ) and charge transfer resistance calculated from EIS spectra ( $R_{\text{CTEIS}}$ )

Specimen	1 <sup>st</sup> phase			2 <sup>nd</sup> phase		
	$R_{\text{pVOL}}$ ( $\Omega \text{ m}^2$ )	$R_{\text{pDC}}$ ( $\Omega \text{ m}^2$ )	$R_{\text{CTEIS}}$ ( $\Omega \text{ m}^2$ )	$R_{\text{pVOL}}$ ( $\Omega \text{ m}^2$ )	$R_{\text{pDC}}$ ( $\Omega \text{ m}^2$ )	$R_{\text{CTEIS}}$ ( $\Omega \text{ m}^2$ )
A	0.0471	0.1247	0.0463	0.0705	0.1157	0.0762
A1	0.0251	0.0786	0.0453	0.0691	0.1253	0.0641
B	0.0124	0.0405	0.0180	0.0172	0.0479	0.0283
C	0.0082	0.0315	0.0075	0.0040	0.0256	0.0043
C1	0.0116	0.0178	0.0086	0.0088	0.0346	0.0106
D	0.0161	0.0431	0.0078	0.0316	0.0637	0.0382
D1	0.0153	0.0394	0.0139	0.0213	0.0495	0.0200
E1	0.0181	0.0178	0.0079	0.0205	0.0233	0.0078
E2	0.0215	0.0169	0.0089	0.0228	0.0352	0.0182
F	0.0093	0.0305	0.0087	0.0057	0.0250	0.0062
F1	0.0094	0.0180	0.0060	0.0077	0.0128	0.0067
F2	0.0165	0.0218	0.0099	0.0135	0.0153	0.0071
G	0.0082	0.0156	0.0062	0.0058	0.0135	0.0054
H	0.0022	0.0466	0.0001	0.0032	0.0478	0.0029
I	0.0019	0.0051	0.0009	0.0005	0.0013	0.0006
I1	0.0057	0.0131	0.0095	0.0026	0.0255	0.0030
J	0.0378	0.0977	0.0410	0.0385	0.0764	0.0481
J1	0.0145	0.0732	0.0272	0.0213	0.0821	0.0464
K	0.0043	0.0057	0.0027	0.0020	0.0058	0.0025
Mg	0.0007	0.0028	0.0008			

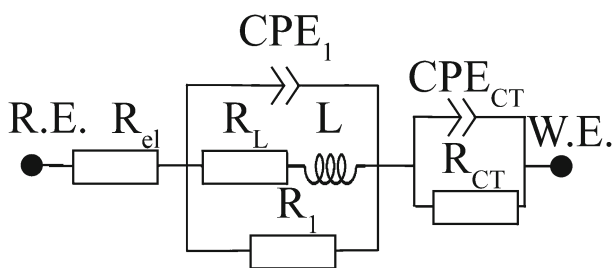


Fig. 2. Equivalent circuit used for EIS spectra analyses.

### 3. Results

The superficial state of specimens after exposures was disparate – from smooth surface with uniform attack to significantly localised corrosion and rough surface. As it was stated above it was not feasible to determine weight changes, given the size and corrosion behaviour of specimens. The data determined with the volumetric method – measurement of released hydrogen – were therefore used as the principal information indicating corrosion behaviour of specimens. Given the two-electron mechanism of magnesium corrosion ( $\text{Mg} = \text{Mg}^{2+} + 2\text{e}$ ), corrosion current  $j_{\text{corr}}$  was determined based on Faraday's law. Polarisation resistances  $R_p$  VOL, summarised in Table 2, were calculated according to the relation  $R_p = B/j_{\text{corr}}$ . Selection of the constant value 0.027 V is explained in the discussion section. In the Table 2, 1<sup>st</sup> phase refers to the behaviour at the end of 5<sup>th</sup> hour and 2<sup>nd</sup> phase refers to the behaviour at the end of 24<sup>th</sup> hour of the exposure. Corrosion rate of magnesium was approximately constant during the entire testing period, data only for the first phase is therefore presented.

Values of polarisation resistances determined by a standard direct current technique are summarised in Table 2.

A regression function derived from an equivalent circuit shown on Fig. 2 was used to analyse EIS spectra of all specimens. This model represents the simplest description of a system where a charge is exchanged on the metal (Me) – layer (l) phase boundary and a layer of corrosion products is formed at the same time. Table 2 summarises resistances corresponding to the corrosion reaction rate ( $R_{CT}$ ) in both measurement phases. Result of fitting process is illustrated in Fig. 3.

XPS measurements were performed on A specimens, which showed the highest corrosion resistance, J samples with an “intermediate“ corrosion behaviour and C alloy from the group of specimens with the highest corrosion rate. The results in wt.% are given in graphs in Fig. 4 so as to enable comparison with the bulk composition of alloys.

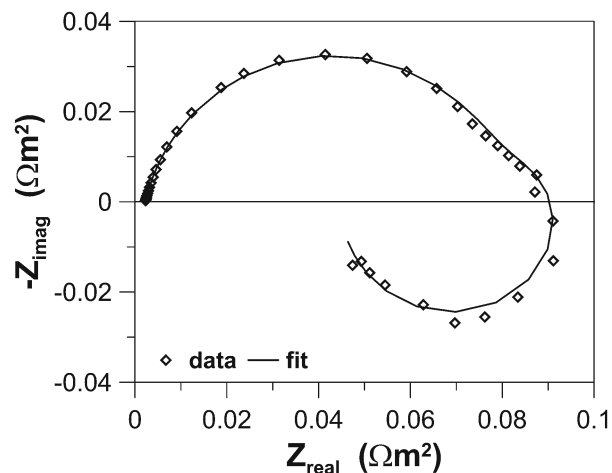


Fig. 3. Electrochemical impedance spectroscopy – example of measured data and result of analysis (sample J1).

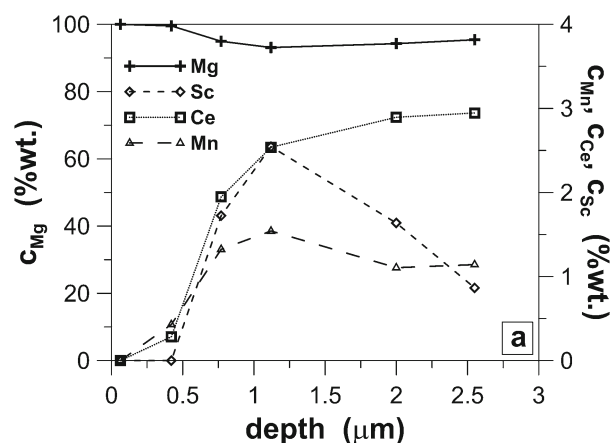


Fig. 4. Depth profiles of magnesium and alloying elements (measured by XPS; a = A, b = J, c = C).

## 4. Discussion

### 4.1. Hydrogen release rate

Division of the measurement into 3 phases and opening of the apparatus in the middle phase for 14 h made it possible to detect the volume of released hydrogen with a sufficient accuracy in initial and final phases. Should the measurement be not performed in this way, a burette with a larger volume would have to be used, which would not only impair the measurement accuracy but would also affect the results by increasing pressure during night hours. Position of the mercury container was changed (manually) from time to time during the measurement so that the atmospheric pressure was constantly maintained within the apparatus. In addition to the unambiguously defined pressure and temperature condi-

tions, the experimental apparatus benefits from the uniform accessibility of the sample surface for electrolyte. It is usually not fully ensured for commonly used apparatuses with a reversed funnel and collection into the fitted burette. The resulted data were fitted with a straight-line with an acceptable accuracy in both phases of exposure, except for a short period of time in the very beginning. The initial phase could have been affected by absorption of hydrogen released in the specimen as a result of the corrosion reaction. The volumetric method results can differ systematically from electrochemical results in a situation when the alloy grains drop out – released hydrogen is not electrochemically detected in this case.

The values of anodic ( $\beta_a$ ) and cathodic ( $\beta_c$ ) slopes of the potential – current density curve (so called Tafel slopes) and the corrosion process mechanism must be known in order to recalculate the volume of released hydrogen to polarisation resistance, the value of which was chosen as a benchmark for the other experimental approaches. The constant  $B = \beta_a\beta_c / [2.303(\beta_a + \beta_c)]$  was calculated based on the works [14–16], where both slopes are summarised in detail. The average value of  $B = 0.027$  V, resulting from the published values, was used for calculations (Table 2). For all specimens in both phases of exposure, the hydrogen release rate was directly proportional to time.

Measurement of the volume of hydrogen released during corrosion exposures was done under unambiguous conditions – the initial exposed surface was well defined, the opening for the sample attachment was properly sealed with Teflon fibre. Temperature and pressure conditions within the apparatus were maintained on the defined/constant level. Considering exchangeable burettes, the apparatus can be well used for comparing corrosion behaviour of various materials.

#### 4.2. Polarisation resistance

In terms of instrumentation, determination of polarisation resistance is a simple method, the electrochemical interpretation of which is also seemingly simple. The problem is that the obtained value of direct current resistance corresponds to the sum of all ohmic contributions within the studied circuit. The determined polarisation resistances were significantly higher compared to the polarisation resistances calculated from the hydrogen release rates. It is clearly visible from the  $R_p\text{DC}/R_p\text{VOL}$  ratio in the second phase of exposure, when the system was definitely in a stationary state, given in Fig. 5. The value for H specimen equalled to 15.1 and is not shown.

#### 4.3. Impedance spectroscopy

The great benefit of the electrochemical imped-

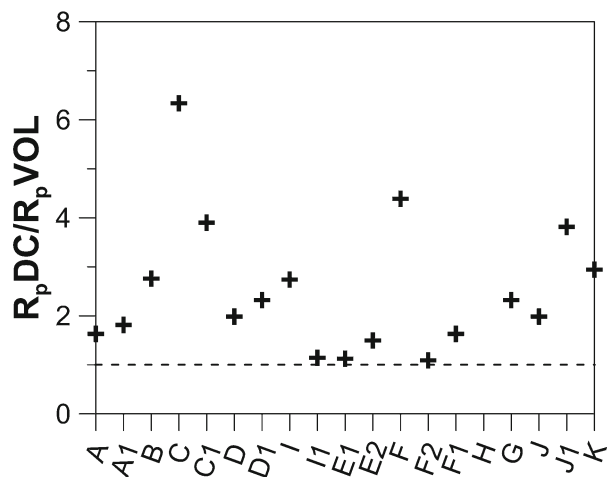


Fig. 5. Ratio of polarisation resistances calculated from release of hydrogen ( $R_p\text{VOL}$ ) and electrochemical measurements ( $R_p\text{DC}$ ).

ance spectra measurement method is that it provides comprehensive information about corrosion behaviour of a material. If there is a physic-chemical model that describes processes on the metal-electrolyte phase boundary, it is possible to implement a more detailed analysis of the corrosion process. The electrochemical impedance spectroscopy has been used in various publications as one of the experimental methods. Magnesium and magnesium alloys spectra are not typical compared to the spectra of most common “corroding” systems measured at the open circuit potential. The difference relates to the presence of so-called inductive loop. This means an area in the low frequency range, in which the phase angle reaches positive values. The inductive component is in this case related to adsorption or precipitation of corrosion products. Various literature sources dealing with magnesium corrosion and corrosion influenced by precipitation of corrosion products suggest a number of equivalent circuits involving several RC members and an inductive component [17–23].

When designing an equivalent circuit modelling the corrosion process on the surface of the exposed specimen, we considered the fact that the photoelectron spectroscopy undoubtedly proved the existence of a rather massive surface layer with a composition differing from the base material. Magnesium ion is the corrosion product at electrolyte’s neutral pH and specimens’ open circuit potential on the level of  $-1.7$  V/SHE [24]. The increase of surface concentration of  $\text{Mg}^{2+}$  ions can be expected during the exposure, which shifts the thermodynamic equilibrium of  $\text{Mg}^{2+}/\text{Mg}(\text{OH})_2$  towards to lower pH [24]. At the same time, considering the proceeding cathodic reaction, pH on the surface of specimens develops to higher levels.  $\text{Mg}(\text{OH})_2$  begins to precipitate if its solubility product is exceeded under the current conditions. XPS concen-

tration profiles of alloy components and microscopic assessment of the superficial state proved that the voluminous layer of corrosion products did not create on specimens with high corrosion resistance. Even in this case though, there was a layer on the surface of specimens, the composition of which differed from the bulk of material. A relatively simple circuit (Fig. 2) was suggested for the EIS spectra analyses, which considered the corrosion reaction and the existence of a layer formed as a result of precipitation of magnesium hydroxide and/or merely corrosion products of alloying elements. Parallel combination of  $R_{CT}$  and  $CPE_{CT}$  describes oxidation on the metal-layer phase boundary. The other part of the equivalent circuit characterises behaviour of the layer. Its properties are described by a parallel combination of  $CPE_1-R_1$  and  $L$  ( $R_L$  being the resistance of an inductive component). In principle, the scheme corresponds to the circuit suggested by the study [25], the arrangement of the members of the scheme shown in Fig. 2 formally reflects succession of the processes. Accuracy of the fit was mostly acceptable with minor deviations between the measured data and the regression function curve (Echem Analyst software goodness of fit on the level of  $1 \times 10^{-4}$ ). Errors in determination of parameters values ranged from units to lower tens of percent.

Values of charge transfer resistances determined on the base of this analysis are close to results of volumetric method more than the polarisation resistance values measured by direct current method as it is obvious from Fig. 6 and Fig. 5 comparison. The sum of resistances  $R_{SUMEIS}$ , which means summarisation of all ohmic components of the equivalent circuit, calculated from the EIS spectra analyses results, are in good agreement with polarisation resistances determined by the DC measurement. This result was expected because  $R_{pDC}$  measurements provided the sum of all resistances within the circuit, not only resistance corresponding with corrosion reaction.

With decreasing corrosion resistance of alloys the resistance of layer increases (Fig. 7). The change of the  $R_1/R_{SUMEIS}$  ratio is less steep in the first phase than in the second phase of exposure. At the same time, it is obvious that the ratio differs from specimen to specimen. Hence the DC polarisation resistance values are burdened by the influence of variability of the layer's resistance contribution.

Compared to the polarisation resistance measurement, the impedance spectroscopy was more successful even in the corrosion behaviour trend monitoring. In the second phase of exposure, both DC and AC method described the trend for six of nineteen studied materials, for five of them no agreement with the measurement of released hydrogen volume was found. For all other materials, the trend was correctly described by the electrochemical impedance spectroscopy.

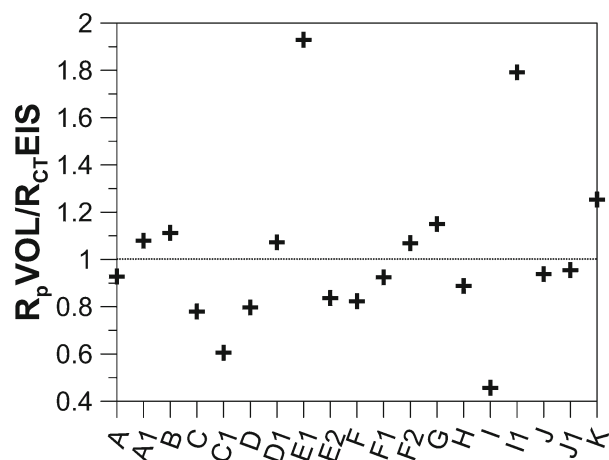


Fig. 6. Ratio of polarisation resistances calculated from release of hydrogen ( $R_p VOL$ ) measurement and EIS impedance spectra analysis ( $R_{CTDC}$ ).

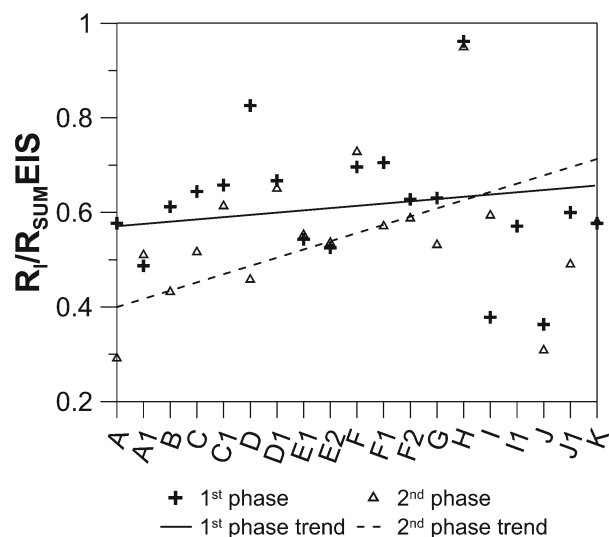


Fig. 7. Ratio of surface layer resistance ( $R_1$ ) and overall sample resistance ( $R_{SUMEIS}$ ) calculated from electrochemical impedance spectra.

## 5. Conclusions

1. An apparatus for measurement of the volume of released hydrogen under clearly defined conditions was designed in the study.

2. Measurement of electrochemical impedance spectra provides more complex information on the system behaviour in comparison with simple polarisation resistance technique. The data can be used to determine both the development of the charge transfer resistance as well as the layer resistance. This represents an important advantage compared to the polarisation resistance determined by the DC technique. The layer

resistance – total resistance ratio ( $R_i/R_{\text{SUMEIS}}$ ) was changing during the measurement, therefore any comparison based only on  $R_{\text{pDC}}$  can be problematic.

3. The quality of corrosion behaviour assessment would substantially be increased by comparing results of several methods.

### Acknowledgement

This work was supported by the Czech Science Foundation – project P108/12/G043.

### References

- [1] Witte, F., Hort, N., Vogt, C., Cohen, S., Kainer, K. U., Willumeit, R., Feyerabend, F.: *Curr Opin Solid St M*, 12, 2008, p. 63. [doi:10.1016/j.cossms.2009.04.001](https://doi.org/10.1016/j.cossms.2009.04.001)
- [2] Feyerabend, F., Drücker, H., Laipple, D., Vogt, C., Stekker, M., Hort, N., Willumeit, R.: *J. Mat. Sci. Materials in Medicine*, 23, 2012, p. 9. [doi:10.1007/s10856-011-4490-5](https://doi.org/10.1007/s10856-011-4490-5)
- [3] Zeng, R., Dietzel, W., Witte, F., Hort, N., Blawert, C.: *Adv. Eng. Materials*, 10, 2008, p. B3. [doi:10.1002/adem.200800035](https://doi.org/10.1002/adem.200800035)
- [4] Kokubo, T., Takadama, H.: *Biomaterials*, 27, 2006, p. 2907. [doi:10.1016/j.biomaterials.2006.01.017](https://doi.org/10.1016/j.biomaterials.2006.01.017)
- [5] Zhang, S., Zhang, X., Zhao, C., Li, J., Song, Y., Xie, C., Tao, H., Zhang, Y., He, Y., Jiang, Y., Bian, Y.: *Acta Biomater.*, 6, 2010, p. 626. [doi:10.1016/j.actbio.2009.06.028](https://doi.org/10.1016/j.actbio.2009.06.028)
- [6] Walker, J., Shadanbaz, S., Kirkland, N. T., Stace, E., Woodfield, T., Staiger, M. P., Dias, G. J.: *J. Biomed. Mater. Res. Part B, Applied Biomaterials*, 100, 2012, p. 1134. [doi:10.1002/jbm.b.32680](https://doi.org/10.1002/jbm.b.32680)
- [7] Kirkland, N. T., Birbilis, N., Staiger, M. P.: *Acta Biomater.*, 8, 2012, p. 925. [doi:10.1016/j.actbio.2011.11.014](https://doi.org/10.1016/j.actbio.2011.11.014)
- [8] Song, G., Atrens, A., St John, D., Wu, X., Nairn, J.: *Corros. Sci.*, 39, 1997, p. 1981. [doi:10.1016/S0010-938X\(97\)00090-5](https://doi.org/10.1016/S0010-938X(97)00090-5)
- [9] Ghoneim, A. A., Fekry, A. M., Ameer, M. A.: *Electrochim. Acta*, 55, 2010, p. 6028. [doi:10.1016/j.electacta.2010.05.062](https://doi.org/10.1016/j.electacta.2010.05.062)
- [10] Pardo, A., Feliu Jr., S., Merino, M. C., Arrabal, R., Matykina, E.: *International Journal of Corrosion*, 2010, 2010, Article ID 953850. [doi:10.1155/2010/953850](https://doi.org/10.1155/2010/953850)
- [11] Zainal Abidin, N. I., Atrens, A. D., Martin, D., Atrens, A.: *Corros. Sci.*, 53, 2011, p. 3542. [doi:10.1016/j.corsci.2011.06.030](https://doi.org/10.1016/j.corsci.2011.06.030)
- [12] Petty, R. L., Davidson, A. W., Kleinberg, J.: *J. Am. Chem. Soc.*, 76, 1954, p. 363. [doi:10.1021/ja01631a013](https://doi.org/10.1021/ja01631a013)
- [13] Grenblatt, J. H.: *J. Electrochem. Soc.*, 103, 1956, p. 539. [doi:10.1149/1.2430151](https://doi.org/10.1149/1.2430151)
- [14] Shi, Z., Atrens, A.: *Corros. Sci.*, 53, 2011, p. 226. [doi:10.1016/j.corsci.2010.09.016](https://doi.org/10.1016/j.corsci.2010.09.016)
- [15] Cai, J., Cao, F., Chang, L., Zheng, J., Zhang, J., Cao, C.: *Appl. Surf. Sci.*, 257, 2011, p. 3804.
- [16] Liu, M., Schmutz, P., Uggowitzer, P. J., Song, G., Atrens, A.: *Corros. Sci.*, 52, 2010, p. 3687. [doi:10.1016/j.corsci.2010.07.019](https://doi.org/10.1016/j.corsci.2010.07.019)
- [17] Anik, M., Celikten, G.: *Corros. Sci.*, 49, 2007, p. 1878. [doi:10.1016/j.corsci.2006.10.016](https://doi.org/10.1016/j.corsci.2006.10.016)
- [18] Xin, Y., Huo, K., Tao, H., Tang, G., Chu, P. K.: *Acta Biomater.*, 4, 2008, p. 2008. [doi:10.1016/j.actbio.2008.05.014](https://doi.org/10.1016/j.actbio.2008.05.014)
- [19] Alvarez-López, M., Pereda, M. D., del Valle, J. A., Fernández-Lorenzo, M., García-Alonso, M. C., Ruano, O. A., Escudero Ricón, M. L.: *Acta Biomater.*, 6, 2010, p. 1763. [doi:10.1016/j.actbio.2009.04.041](https://doi.org/10.1016/j.actbio.2009.04.041)
- [20] Mosialek, M., Mordarski, G., Nowak, P., Simka, W., Nawrat, G., Hanke, M., Socha, R. P., Michalska, J.: *Surf. Coat. Technol.*, 206, 2011, p. 51. [doi:10.1016/j.surfcoat.2011.06.035](https://doi.org/10.1016/j.surfcoat.2011.06.035)
- [21] Lei, T., Tang, W., Cai, S.-H., Feng, F.-F., Li, N.-F.: *Corros. Sci.*, 54, 2012, p. 270. [doi:10.1016/j.corsci.2011.09.027](https://doi.org/10.1016/j.corsci.2011.09.027)
- [22] Zheng, Y. F., Gu, X. N., Xi, Y. L., Chai, D. L.: *Acta Biomater.*, 6, 2010, p. 1783. [doi:10.1016/j.actbio.2009.10.009](https://doi.org/10.1016/j.actbio.2009.10.009)
- [23] Qu, Q., Ma, J., Wang, L., Li, L., Bai, W., Ding, Z.: *Corros. Sci.*, 53, 2011, p. 1186. [doi:10.1016/j.corsci.2010.12.014](https://doi.org/10.1016/j.corsci.2010.12.014)
- [24] Pourbaix, M.: *Atlas of Electrochemical Equilibria in Aqueous Solutions*. Houston, NACE 1974.
- [25] Jamesh, M., Kumar, S., Sankara Naranzan, T. S. N.: *Corros. Sci.*, 53, 2011, p. 645. [doi:10.1016/j.corsci.2010.10.011](https://doi.org/10.1016/j.corsci.2010.10.011)